Fourier Transform Infrared Microspectroscopy of Phase-Separated Mixed Biopolymer Gels

C. Matin Durrani and Athene M. Donald*

Department of Physics, Cavendish Laboratory, University of Cambridge, Madingley Road, Cambridge CB3 0HE, U.K.

Received May 18, 1993; Revised Manuscript Received October 12, 1993®

ABSTRACT: We present results which show how Fourier transform infrared (FTIR) microspectroscopy can be used as a valuable tool in the study of phase-separated mixed biopolymer solutions and gels. The work in this paper deals specifically with the ternary amylopectin–gelatin–D_2O system which forms thermoreversible gels when a hot mixed solution is cooled to room temperature. First, we show how the integrated area of particular infrared absorption peaks from the two polymers can be used as an estimate for composition, and we use this approach to monitor the spatial fluctuations in composition by tracking across a sample and also to monitor changes in composition with time at fixed position. We also use this approach to establish the scale upon which phase separation takes place by taking the infrared spectrum over a range of sampling sizes at fixed position. Second, we use FTIR microspectroscopy coupled with partial least-squares analysis to determine quantitatively polymer concentration in the micro-phase-separated domains of a mixed gel. From a comparison of these concentrations with the previously determined equilibrium phase diagram of this system, we find that for samples held for long enough above the gelation temperature of either component before quenching, the concentration in the phase-separated domains of the gel are the same as those found at equilibrium in the liquid–liquid bulk phase-separated phases.

Introduction

Gelation is a widely studied phenomenon in polymer science and is encountered with both synthetic and biological polymers. A polymer gel is a three-dimensional network of chains, held together through cross-links. Most biopolymer gels are termed "physical" gels because they have physical cross-links, known as junction zones, which extend across portions of the chain.[1] These zones hold the chains together through physical forces such as Coulombic interactions, dipole–dipole interactions, and hydrogen or van der Waals bonding. Examples of junction zones include the double helices in gels from the polysaccharide agar, the triple helices in gelatin gels, and the ion-mediated junction zones in alginate where divalent calcium ions occupy sites between laterally associated regions of chain.[2] Physical gels, including those studied in this paper, are usually thermoreversible and differ from chemically cross-linked gels, whose cross-links are permanent pointlike covalent bonds.

Although gels and gelation processes have been extensively investigated over the years, most effort has understandably been directed toward single polymer gels. The gelation of mixtures of biopolymers in solution is a more complicated affair that has remained largely unexplored. Mixtures of biopolymers in aqueous solution have however become of increasing importance to the food industry in the search for food materials with new characteristics of texture and rheology. Their behavior has therefore attracted growing interest in recent years,[3] and it is this interest that has motivated our work.

The way in which a mixture of gel-forming biopolymers in solution behaves is complicated by the fact that mixtures of polymers tend to be immiscible. The consequence of this immiscibility is that if a mixed biopolymer solution of sufficient concentration is held above the gelation temperature of either component, liquid–liquid phase separation occurs. Density differences between the phases may eventually lead to the creation of two bulk phases. However, when a mixed biopolymer solution containing gel-forming polymers is cooled below the gel temperature of either or both components, phase separation and gelation become competing processes and several alternative gel microstructures are possible. The resultant structure depends not only on the nature of the polymers themselves but also on the degree of miscibility of polymers in solution, the relative time scales of phase separation and gelation, and the thermal history to which the mixture is subjected. Brownsey and Morris[4] laid down three different categories for mixed gels which are summarized as follows:

(i) Coupled Networks. In these mixed gels the junction zones are formed through specific, favorable synergistic interactions between stretches of compatible regions of different chains, with the result that a single gel network is formed. It has been proposed that xanthan forms a coupled network with carob-galactomannan[5] and also with tara-galactomannan.[6]

(ii) Interpenetrating Networks. This term is used to describe a gel in which one polymer forms a secondary network within the confines of the other polymer's network. Evidence for such gels is difficult to extract experimentally but, despite some controversy in the literature, it appears that the carageenan/carobgalactomannan mixed gel belongs to this category.[7]

(iii) Phase-Separated Gels. A phase-separated mixed gel consists of a continuous supporting phase containing inclusions of the other phase. These systems have a phase inversion at a particular concentration at which the predominant component in the continuous and supporting phases changes over.

Despite the presence of a large volume fraction of solvent (water), there are analogies and structural similarities between mixed gels and conventional polymer blends. This led Clark et al.[8] to develop a model to describe the relationship between the modulus of a phase-separated mixed gel and the concentrations of the two component polymers in each phase on the basis of Takayanagi's approach to the calculation of the modulus of a binary polymer blend. In the Takayanagi model, the modulus of the composite material is not explicitly calculated for each polymer volume fraction ratio, instead upper and lower

® Abstract published in *Advance ACS Abstracts*, December 1, 1993.

0024-9297/94/2227-0110$04.50/0

(isostrain and isostress) bounds for the modulus are established. However the Takayanagi treatment is intended to describe a blend that contains pure, mutually insoluble components: one of the difficulties any model for mixed gels has to contend with lies in the presence of solvent and in the uncertainty of how the solvent partitions itself between the two phases. Clark et al.[8] assumed that there was complete absence of one polymer in the other's phase and then used a parameter to describe the relative affinity of the two phases for solvent. However, we have determined the equilibrium phase diagram of the amylopectin–gelatin–D_2O system which showed that complete demixing did not occur, in this system at least. Thus there is reason to question the assumption made by Clark et al. that complete demixing occurs in the gel.

One of the main difficulties in the study of phase-separated mixed aqueous biopolymer systems lies in the fact that any phase separation is difficult to detect, unless it occurs on a bulk scale through the formation of two distinct layers. The detection of individually phase-separated regions in an apparently macroscopically single-phase system is not possible either by visual inspection or by optical microscopy if the refractive indices of the two component polymers in solution are not significantly different. In instances when this condition is not met, then it is possible: phase-separated dextran rich droplets in amylose/dextran solutions held at 75 °C and amylopectin-rich droplets in amylose/amylopectin solutions held at 80 °C have been observed.[10] One method to skirt the difficulty of there not being any visual distinction between phases has been to use staining techniques to detect the presence of one of the polymers. Clark et al.[8] used tannic acid, glutaraldehyde, and osmium tetraoxide to stain gelatin preferentially in gelatin/agar mixed gels. Horiuchi and Sugiyama[11] used toluidine blue to stain the agar in gelatin/agar mixed gels and combined this with phase-contrast microscopy—a technique which can help to identify the phases visually.

Even if the phases in a mixed gel can be observed, it has proved difficult to determine the compositions in the phases with any precision. Doi[12] used the degree of iodine coloration to estimate qualitatively the degree of phase separation in amylopectin/gelatin mixed gels. In their work on gelatin/agar mixed gels, Horiuchi and Sugiyama[11] used a microspectrophotometer, in combination with the phase-contrast microscope, to monitor the absorption of visible light between 400 and 700 nm by selected regions in a mixed gel. This provided only semiquantitative results because it relied on measuring the differences in absorption in the two phases over and above that of the toluidine blue which absorbed in the same region as gelatin. They found, for example, that droplets of agar-rich regions were "almost all" agar—in agreement with work by Clark et al. on agar/gelatin mixed gels[8]—and that the medium in which the droplets were held was considered to consist not only of gelatin but also of agar, in a ratio "somewhat lower" than in the droplets. However until now there had been no technique which allowed direct experimental determination of phase composition in such gels.[13] Morris[13] stresses that with no other evidence forthcoming, it can only be assumed that there is no "cross-contamination" between the phases; i.e. complete phase separation occurs. This has recently been shown not to be the case in a bulk phase separated system,[14] but the question remains whether this translates to the situation below the gelation temperature. In this paper, Fourier transform infrared (FTIR) microspectroscopy is used to investigate this question. Although Morris[13] suggests that new techniques such as laser–Raman microscopy and scanning tunnelling microscopy may eventually allow determination of phase composition, FTIR microspectroscopy is shown in this paper to be capable of the task.

FTIR microspectroscopy is a microanalytical technique which interfaces an FTIR spectrometer to an optical microscope.[15,16] It enables the infrared spectrum of sampling regions of variable size, down to a practical limit of about 10-μm resolution, to be taken. Consequently, FTIR microspectroscopy is ideal for compositional mapping and analysis in heterogeneous samples whose domain sizes are in the tens of micrometer range.[17]

We identified four types of experiments which could be conducted with an FTIR microscope to study mixed-polymer solutions and gels. The first three are comparatively straightforward in that the integrated area of particular infrared absorption peaks is simply used as a measure of composition of the two polymers. The fourth type of experiment involves making quantitative predictions for the actual concentrations of the two polymers on the basis of a calibration set of infrared spectra from samples of known concentration.

(i) The spatial variation of composition in a sample can be established by taking the infrared spectrum at successive adjacent positions in the sample and measuring the area of infrared absorption peaks from the two polymers at each position. This procedure is used to detect any phase separation which cannot be observed optically and to verify that one-phase samples are indeed homogeneous.

(ii) Time-related changes in composition can be investigated by monitoring the infrared peak areas from sequentially acquired spectra at a fixed position in the sample. This can be used to monitor, for example, the kinetics of phase separation of an initially homogeneous liquid, or to see if the composition of a phase-separated domain changes once a phase-separated structure has been formed.

(iii) The size of phase-separated regions can be estimated by taking the infrared spectrum over a range of apertured areas at the same position in the sample. The infrared spectrum will depend on the ratio of the sampled area to the size of the phase-separated region. As the apertured area is reduced in size, the area of the infrared absorption peaks will change if a phase-separated region rich in one polymer and deficient in the other begins to dominate the field of view. This approach has been adopted previously in the study of fluid inclusions in geological minerals[18] but is similarly relevant here.

(iv) Although the measurement of peak areas is a convenient way of monitoring composition, the peak areas calculated in this way are only relative and do not give an absolute value of concentration. To determine quantitatively the biopolymer concentration at particular regions in the sample, the statistical analytical technique of partial least-squares (PLS) analysis is used. This technique is based on taking the infrared spectra from samples of known composition to predict the concentrations in spectra of unknown composition.

The work in this paper deals with the amylopectin–gelatin–D_2O system which is a biopolymer mixture with strong industrial relevance. Amylopectin is a highly and nonrandomly branched polysaccharide derived from starch. It forms crystalline gels upon cooling the hot amylopectin solution to below room temperature. Its gelation mechanism is complicated and has been the subject of investigation by us and only few other researchers.[19] In contrast, gelatin gelation has been extensively studied and it is well

known that this linear protein forms gels upon cooling solutions as dilute as 1% (w/w) to below 35 °C.[20] The biopolymers used were the same ones studied earlier by us.[14] In that paper we described a general method using FTIR spectroscopy to determine the concentrations in the liquid–liquid bulk separated phases of a mixed aqueous biopolymer system held at a temperature (51 °C) above the gelation temperature of the polymers. The results from the method were used to plot out the phase diagram of the amylopectin–gelatin–D_2O system at 51 °C. The work in this paper uses FTIR microspectroscopy to investigate phase-separated amylopectin–gelatin–D_2O mixed solutions held at 51 °C and gels formed by cooling to 28 °C from 51 °C. The rationale behind the use of D_2O was given in our earlier work[14] and is based on the fact that, if water is used, many of the key absorption bands of the two biopolymers are obscured by the strong absorption of H_2O in the form of an O–H stretch between 1600 and 1800 cm^{-1}.

Experimental Section

Instrumentation. Commercially available FTIR microscopes are modified research-grade optical microscopes which have been adapted for use in either infrared or optical mode. In this work a Spectra Tech IR-PLAN microscope was used; it is a modification of the Olympus BH2 MJLT microscope. Infrared radiation entered the microscope from a Mattson 40-20 Galaxy FTIR spectrometer. Detection of the infrared radiation was by a narrow-band mercury–cadmium–telluride detector between 740 and 5000 cm^{-1}. The ×15 objective and ×10 condenser lenses in the microscope are non-infrared-absorbing Cassegrainian lenses. They are constructed from front surface mirrors and are mounted on-axis so that the path for the visible light is parfocal and colinear with the infrared light.

The microscope stage of the IR-PLAN was moveable in both the x and y directions and was controlled by a Vernier scale with a resolution of 100 μm. Regions of interest in the sample were spatially isolated using the microscope's apertures. The sample is not physically apertured since the actual physical position of the apertures is not in or near the sample plane. Instead, using the technique known as redundant aperturing, the two apertures take up positions in the microscope such that their images coincide in the sample plane.[21] Both apertures consisted of a set of crossed knife blades which allowed areas of interest to be delineated by a rectangle of adjustable size. A pair of circular apertures of fixed 100-μm diameter was also used in some of the experiments to delineate regions of interest. The microscope was purged free of most water vapor and carbon dioxide by constructing an airtight perspex box which completely enclosed the whole microscope and detector chamber, through which dried, carbon dioxide-free compressed air was passed at a rate of 300 L min^{-1}.

Sample Preparation. A sample cell containing two 2-mm-thick silver chloride windows was used in all the microscopy experiments; resistors on the underside of the cell mounting enabled the sample temperature to be controlled. The mean cell path length was calculated by measuring the fringe spacing of the empty cell placed in the spectrometer; the path length could be altered by adjusting the tightness of screws which clamped the cell together. The upper limit to sample thickness was found to be ~25 μm, but typical sample thicknesses in this work lay between ~12 and 20-μm.

The samples were prepared on a weight percentage basis by weighing out the appropriate masses of amylopectin, gelatin, and D_2O into a sealed bottle. Samples were left overnight at room temperature to allow the gelatin to swell and were then heated to 85 °C for 10 min while being mixed with a magnetic stirring bar. With the use of 1-mL disposable syringes, the hot solution was injected into the cell and set to a temperature of 51 °C, between the two windows. Samples were studied either at 51 °C or cooled in the cell naturally, according to Newton's law of cooling, to room temperature to allow gelation to occur.

All spectra were taken at 8-cm^{-1} resolution and the interferograms were coadded and Fourier transformed using Beer–Norton Strong apodization. A spectrum of a pair of 2-mm silver chloride windows clamped together was used as background. For those experiments in which samples were studied over a range of aperture sizes, in order to compensate for the decrease in signal throughput as the apertured area was successively reduced, the number of scans taken were selected to try to achieve approximately the same signal-to-noise ratio throughout.

Phase-separated regions could be detected visually, provided the sample was held between optically transparent calcium fluoride windows and that the sample was viewed under the superior image contrast of a Jenapol optical microscope. Unfortunately the infrared emissivity of calcium fluoride goes to zero in the FTIR microscope at 1040 cm^{-1}. Calcium fluoride windows could therefore not be used to generate results with the FTIR microscope since important amylopectin absorption peaks which occur in this region of the spectrum were lost. Silver chloride however continues to be transparent to infrared down to 350 cm^{-1} and was therefore chosen as a window material. However, the optical opacity of silver chloride prevented any visual detection of phase-separated regions in the FTIR microscope. Optical micrographs were taken in the Jenapol optical microscope with the sample confined between calcium fluoride windows and serve in this paper merely as a comparison and verification of the scale of phase separation detected using the FTIR microscope.

Data Handling. The data were treated in the manner we used in our earlier work:[14] to account for the possible variation in sample thickness at different positions in the samples, each infrared spectrum was normalized by setting the lowest point in the region 800–1800 cm^{-1} to zero and scaled so that the D_2O peak at 1212 cm^{-1} was unity. Estimates for the amount of gelatin and amylopectin relative to the amount of D_2O were made by integrating the area beneath the gelatin amide I band between 1600 and 1723 cm^{-1} and beneath the amylopectin peak from C–C and C–O vibrations between 987 and 1120 cm^{-1}. The integrations were performed to a linear baseline using FIRST software supplied by Mattson.

Partial Least-Squares Analysis. To determine the biopolymer concentration quantitatively at particular regions in the sample, the partial least-squares (PLS) analysis approach to concentration prediction was adopted. We based our method on the one which has been previously described by us in detail.[14] In the PLS approach, spectra from a series of calibration samples of known concentration are used to form a matrix of calibration spectra of intensity at each experimentally sampled frequency which is then used to predict concentration from the spectrum of a sample of unknown concentration. To use the PLS approach to concentration prediction with FTIR microspectroscopy, the calibration spectra have to be taken at one particular aperture size (because infrared absorption and baseline may change with area size), and this size must be the same for both the standards and the unknown mixtures. Performing quantitative experiments with an FTIR microscope also requires that the apertured area of the sample be precisely the same as that of the background.[22] This meant that when the spectrum of the sample had been taken, no adjustment to the apertures was permissible once the background cell was in place. Great emphasis was therefore placed on ensuring that once the background cell was placed back on the microscope stage, the image of the lower aperture was still centered on the cross hairs of the eyepiece. Spectra from 40-μm × 40-μm regions in a series of 15 calibration samples of known concentrations were obtained to create a calibration matrix of infrared spectra. All the standards, apart from the pure D_2O spectrum, consisted of just single-component polymer solutions: this was to prevent any complications arising from the possible fluctuations in concentration of a mixed polymer standard on a scale less than 40-μm × 40-μm during the course of a measurement. Each spectrum consisted of 25 000 scans of the sample at room temperature, with the empty silver chloride cell as background. All spectra were truncated in the range 800 to 1800 cm^{-1} and scaled so that the D_2O peak at 1212 cm^{-1} was unity. Figure 1 shows two of the calibration spectra and a typical spectrum from a 40-μm × 40-μm region in a sample of unknown concentration. By using FIRST software, the 15 calibration spectra which formed the calibration matrix were then used for the prediction of the amylopectin/D_2O and the gelatin/D_2O ratios

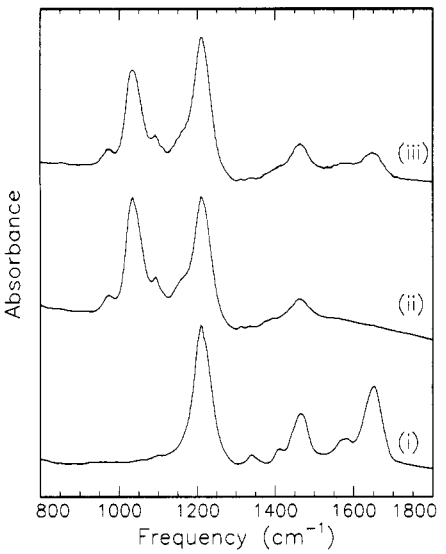

Figure 1. Fourier transform infrared spectra taken with the infrared microscope from 40-μm × 40-μm apertured regions of (i) gelatin in D_2O (11.6% (w/w)); (ii) amylopectin in D_2O (20.1% (w/w)); (iii) an amylopectin-rich phase-separated region of a mixed amylopectin/gelatin gel whose overall concentration was 10% (w/w) amylopectin, 7% (w/w) gelatin, and 83% (w/w) D_2O. All three spectra are shown in the form in which they were used throughout this work, with the lowest point in the region between 800 and 1800 cm^{-1} having been set to zero and the data having been scaled so that the D_2O peak at 1212 cm^{-1} was set to an absorbance of unity.

Table 1. Weight Percentage Concentrations of Samples A–C and Whether They Lie in the One-Phase or the Two-Phase Region of the Phase Diagram (See Figure 2)[a]

sample	concentration, % amylopectin	gelatin	D_2O	one-phase or two-phase
A	10.0	7.0	83.0	two
B	1.9	2.0	96.1	one
C	8.0	6.0	84.0	two

[a] In the case of sample C, it was allowed to bulk phase separate into two liquid layers at 51 °C; only the upper layer was studied (see Figure 5).

from the infrared spectra of 40-μm × 40-μm regions in phase-separated mixed amylopectin/gelatin gels. From the two ratios, by conservation of mass, the concentration of amylopectin, gelatin, and D_2O were determined.

Results

Spatial Concentration Variation. When the infrared microscope was used to scan across a sample, the integrated areas of the infrared absorption peaks of the spectrum taken at each position were used to monitor the changes in composition. This approach revealed the differences between samples falling in the one-phase and the two-phase regions of the phase diagram. Three samples were studied in this manner. Their weight percentage concentrations are given in Table 1 and their positions on the equilibrium-phase diagram for this system are shown in Figure 2. The spectra were taken through 100-μm-diameter circular apertures in steps of 100 μm, with the sample held at 51 °C, i.e. above the gelation temperature of either polymer. Each spectrum consisted of 100 co-added scans. Figure 3 shows the variation in amylopectin and gelatin peak areas at 100-μm intervals for a 10% amylopectin/7% gelatin mixture in the two-phase region of the phase diagram (sample A). There are fluctuations in concentration, in which each position which is amylopectin-rich, is deficient in gelatin, and vice versa. Clearly sample A consists of phase-separated regions, in which

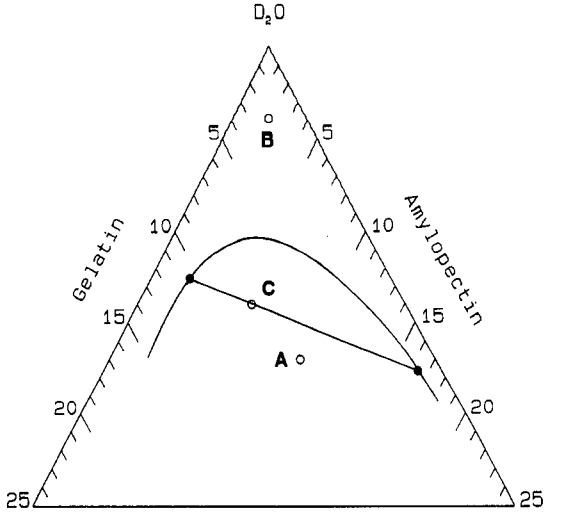

Figure 2. The weight percentage concentrations of samples A–C (O) are shown on a ternary diagram. In the case of sample C, which was allowed to bulk phase separate at 51 °C, the concentration of the upper phase (11%/2%/7%) which was studied and the lower phase (which was not studied) are indicated by filled circles (●). Also shown, for comparison purposes, is the phase diagram for this system at 51 °C established using FTIR spectroscopy. (The phase diagram is taken from Figure 4 in ref 14; a fuller account of how it was determined is given therein.) (Reprinted with permission from ref 14. Copyright 1993 American Chemical Society.)

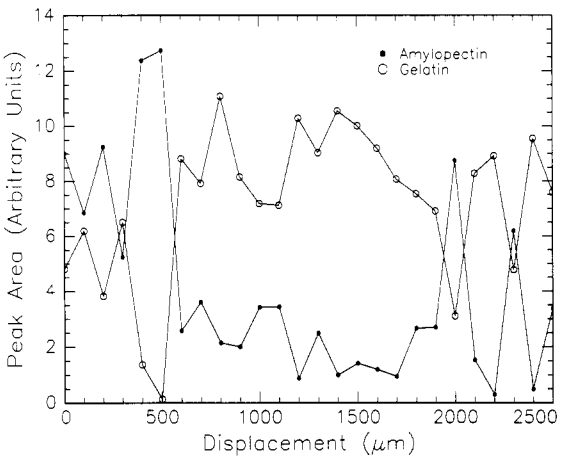

Figure 3. Spatial variation of the integrated area of the amylopectin infrared absorption peak between 987 and 1120 cm^{-1} (●) and of the integrated area of the gelatin infrared absorption peak between 1600 and 1723 cm^{-1} (○) at 51 °C in sample A, a mixture in the two-phase region of the phase diagram.

one or other polymer dominates. That this is a real effect is confirmed by sample B, a 1.9% amylopectin/2.0% gelatin mixture in the one-phase region of the phase diagram, whose fluctuations in composition at 51 °C were much smaller than in sample A and varied in a random fashion from point to point (Figure 4).

In contrast to sample A, Figure 5 shows the variation in composition of the upper phase of an 8.0% amylopectin/6.0% gelatin mixture (sample C) which was kept in a sealed vial placed in an oven at 51 °C and allowed to phase separate into two bulk phases. The mixture was left for ~79 h to ensure equilibrium concentrations in the two phases had been reached. As expected for a sample which had reached equilibrium, the peak areas were approximately spatially invariant, with the small amount of fluctuation in peak areas being significantly less than for samples A or B and without correlation in the variation from point to point. The small fluctuations can be attributed to the effects of noise and imperfect background subtraction.

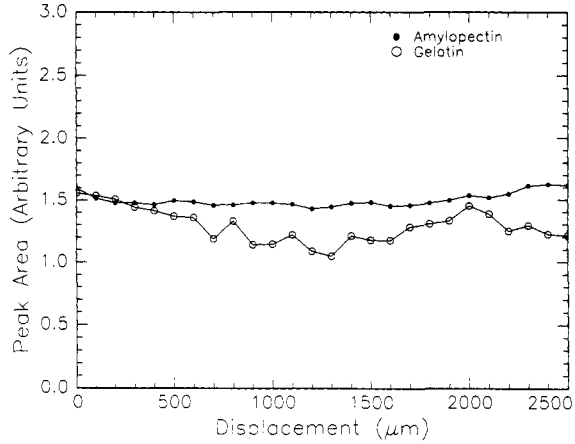

Figure 4. Spatial variation of the integrated area of the amylopectin infrared absorption peak between 987 and 1120 cm^{-1} (●) and of the integrated area of the gelatin infrared absorption peak between 1600 and 1723 cm^{-1} (○) at 51 °C in sample B, a 1.9% amylopectin/2.0% gelatin/96.1% D_2O mixture in the one-phase region of the phase diagram.

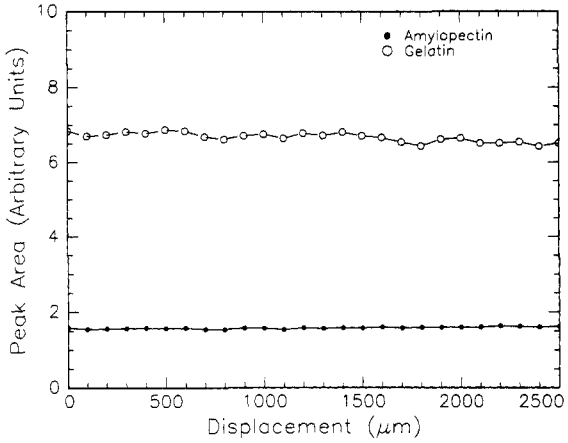

Figure 5. Spatial variation of the integrated area of the amylopectin infrared absorption peak between 987 and 1120 cm^{-1} (●) and of the integrated area of the gelatin infrared absorption peak between 1600 and 1723 cm^{-1} (○) at 51 °C in the upper phase of sample C, an 8.0% amylopectin/6.0% gelatin/84.0% D_2O bulk phase-separated mixture held for 72 h at 51 °C. The concentration of this upper phase was determined to be 11.1% gelatin, 2.0% amylopectin, and 86.9% gelatin using the method described in ref 14.

Interestingly, a sample which was in the one-phase region but which lay close to the phase boundary (4.4% amylopectin/3.8% gelatin) also showed fluctuations which varied between amylopectin- and gelatin-rich regions, although these fluctuations were smaller than those in sample A. Such spatial fluctuations in concentration for samples close to the phase boundary have also been observed in mixtures of dextran and polyethylene glycol in water:[23] this was attributed to preferential interactions between segments of polymers of the same type favoring the formation of microstructures rich in one polymer or the other but whose lifetimes, however, were not long enough to lead to complete separation into two phases.

Sampling over Time at Fixed Position. Experiments on three samples are described to illustrate the effect of sampling in the same fixed position. Again the integrated areas of the infrared absorption peaks were used as a measure of composition. In each case spectra were taken at 1-min intervals over a 100-μm × 100-μm sample area, with each spectrum consisting of 100 co-added scans. Figure 6 shows the time dependence of the gelatin and amylopectin peak areas for a 10% amylopectin/7% gelatin

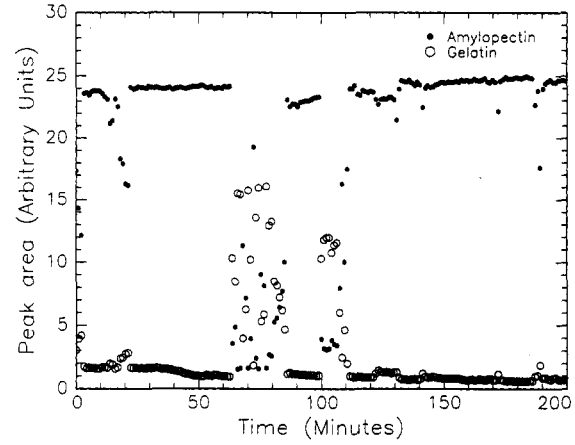

Figure 6. Time variation of the integrated area of the amylopectin infrared absorption peak between 987 and 1120 cm^{-1} (●) and of the integrated area of the gelatin infrared absorption peak between 1600 and 1723 cm^{-1} (○) at 51 °C in a 10% amylopectin/7% gelatin/83% D_2O mixture lying in the two-phase region of the phase diagram.

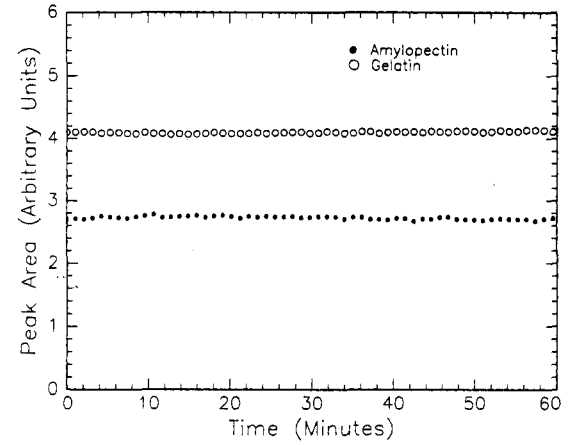

Figure 7. Time variation of the integrated area of the amylopectin infrared absorption peak between 987 and 1120 cm^{-1} (●) and the integrated area of the gelatin infrared absorption peak between 1600 and 1723 cm^{-1} (○) at 51 °C in a 3.5% amylopectin/3.5% gelatin/93% D_2O mixture lying in the one-phase region of the phase diagram.

mixture held at 51 °C, lying in the two-phase region of the phase diagram. The amylopectin and gelatin peak areas appear to exist at two extremes: an abundance of amylopectin is detected whenever there is a deficit of gelatin and vice versa, although some points fell in between. In contrast, the same measurements at 51 °C for a 3.5% amylopectin/3.5% gelatin mixture lying in the 1-phase region of the phase diagram showed peak areas which remained essentially constant with time (Figure 7). This time invariability of the peak areas at fixed position in the one-phase sample implies that the temporal fluctuations in the peak areas at fixed position in the cell for the 10% amylopectin/7% gelatin sample (Figure 6) were not an artifact of the measuring technique but a consequence of the sample being biphasic. The origin of these fluctuations lies in the motion of the sample in the cell at the temperature of 51 °C so that different domains migrate across the field of view.

However it was found that when a 10% amylopectin/7% gelatin sample was held at 51 °C for 30 min before being cooled naturally to 28 °C, the fluctuations in peak area continued while the sample was at 51 °C but disappeared as it was cooled to room temperature (Figure 8). Confirmation that the disappearance of the fluctuations was a permanent effect once a mixture was cooled

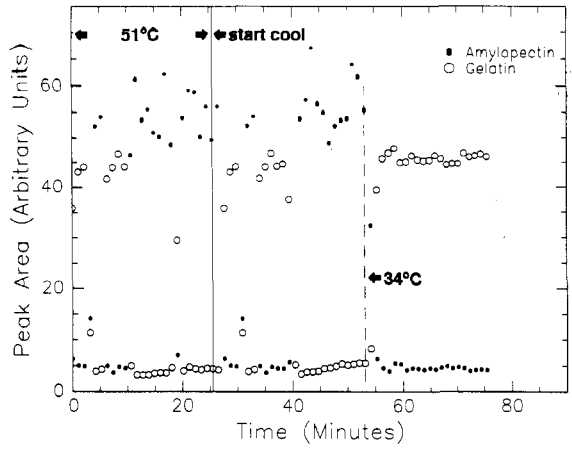

Figure 8. Temporal variation of the integrated area of the amylopectin infrared absorption peak between 987 and 1120 cm^{-1} (●) and of the integrated area of the gelatin infrared absorption peak between 1600 and 1723 cm^{-1} (○) in a 10% amylopectin/7% gelatin/83% D_2O mixture, lying in the two-phase region of the phase diagram. The sample was (i) held at 51 °C for 25 min and then (ii) cooled to 28 °C. The plain vertical line shows the time at which cooling started and the dashed line shows when the sample temperature reached 34 °C, at which the fluctuations disappeared.

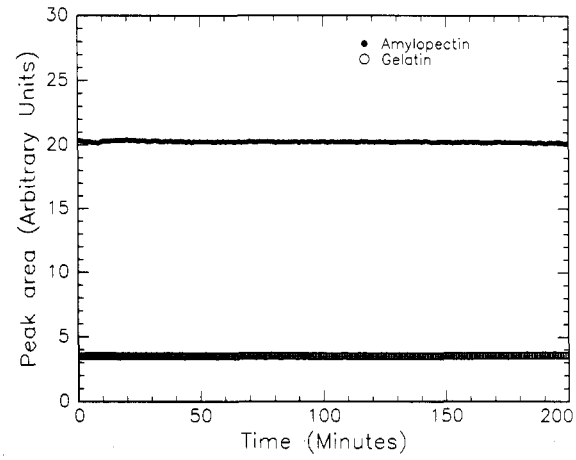

Figure 9. The integrated area of the amylopectin infrared absorption peak between 987 and 1120 cm^{-1} (●) and the integrated area of the gelatin infrared absorption peak between 1600 and 1723 cm^{-1} (○) in a 10% amylopectin/7% gelatin/83% D_2O mixture in the two-phase region of the phase diagram. The sample was held at 28 °C throughout, having been cooled prior to measurement from 51 °C.

naturally from 51 °C is shown in figure 9 in the constancy in peak areas measured continuously at 28 °C for another 10% amylopectin/7% gelatin sample. Since the disappearance in concentration fluctuations occurred at a temperature of 34 °C (Figure 8) and since this temperature corresponded within 1 °C to the gel-formation temperature of gelatin,[20,24] the occurrence of gelatin gelation in the system can account for the freezing-in of the composition.

Effect of Sampling at Different Aperture Sizes. By sampling with different aperture sizes at the same position in the sample and measuring the integrated areas beneath infrared absorption peaks, it is possible to estimate the approximate size of phase-separated regions. This approach was adopted for a 10% amylopectin/7% gelatin mixture held for 25 min at 51 °C and cooled naturally over 45 min to 28 °C. The integrated peak areas from the infrared spectra taken at one position in the sample are shown in Figure 10. At large sampling area (A_1), between 80 μm × 80 μm and 200 μm × 200 μm, the integrated peak areas were essentially constant. As the sampling area was reduced, the area of the amylopectin peak increased at

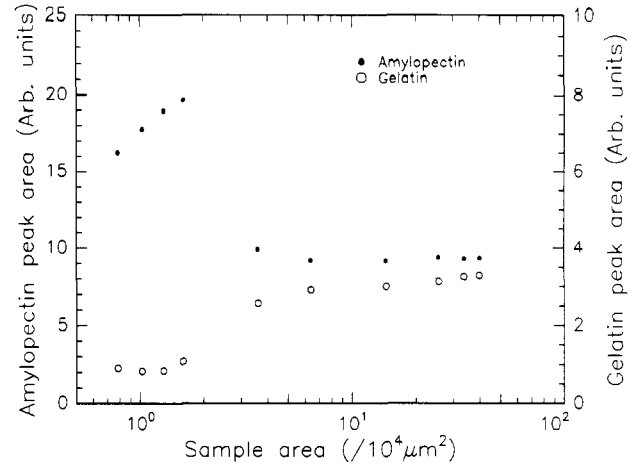

Figure 10. The integrated area of the amylopectin infrared absorption peak between 987 and 1120 cm^{-1} (●) and the gelatin infrared absorption peak between 1600 and 1723 cm^{-1} (○) from spectra taken over a range of square aperture sizes between 200 μm × 200 μm and 28 μm × 28 μm at the same position in a 10% amylopectin/7% gelatin/83% D_2O mixed gel. The sample was held at 51 °C for 25 min and then cooled to 28 °C over 45 min prior to measurement.

the expense of the gelatin peak. At very small sampling areas, the area of the gelatin peak than appeared to reach a plateau, although the amylopectin peak area continued to decrease in size.

These results indicate that above 80 μm × 80 μm the spectra from which the peak areas were calculated were "global" averages and indicative of the average composition in the sample. Hence $A_1/A_2 > 1$ where A_2 is area of the phase-separated region of interest (Figure 11a). Below 80 μm × 80 μm, it can be inferred that an amylopectin-rich phase-separated region was beginning to dominate the spectrum, although some of the surrounding "matrix" will also have been included (Figure 11b). Once the apertured region was small enough—at 40 μm × 40 μm and below—only the phase-separated region of interest was included in the apertured area ($A_1/A_2 < 1$) (Figure 11c). The area A_1 should be the same as the aperture setting below which a reduction in aperture size no longer causes a change in the peak areas.

From the area at which the gelatin peak reached a plateau, A_2 can be estimated to be at least 1600 μm^2 (40 μm × 40 μm). However, the amylopectin absorbance in fact decreased at particularly small aperture sizes. This can be attributed to the onset of diffraction effects. Diffraction occurs when the infrared source passes through the upper aperture, when it is focused from the aperture to the sample plane by the objective, and also at the sample; light which has passed through the sample also gets diffracted by the condenser and by the lower aperture itself.[21] Diffraction is however only significant when the aperture dimensions approach the wavelength of infrared radiation (2–25 μm). The main effect of diffraction is that at small aperture sizes, light spreads outside the specified, apertured area into the surrounding region. This problem is normally exacerbated by the low amount of signal which passes through the apertures at very small aperture sizes. The two effects combined to produce absorption peaks which, despite lengthy acquisition times, became noisy and distinctly non-Gaussian in shape at low wavenumbers in those spectra taken from sampling areas of 32 μm × 32 μm and below. It is clear that, at a given aperture size, diffraction is more significant for infrared absorptions which occur at higher wavelengths: it is therefore likely that the consequences of diffraction were more significant

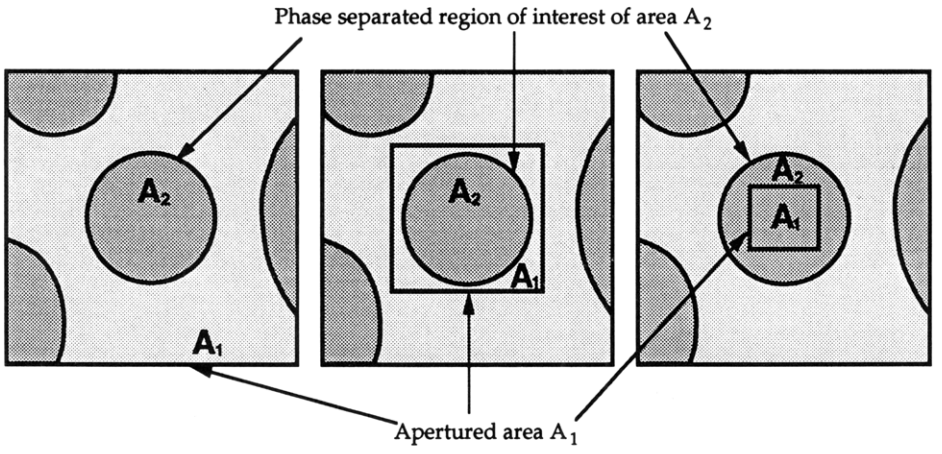

Figure 11. Schematic representation showing how the infrared spectrum taken with an FTIR microscope depends on the ratio of the aperture size, A_1, to the area of the phase separated region, A_2. The darker regions indicate phase-separated domains rich in one polymer and the lighter region indicates the continuous matrix rich in the other polymer. Three cases are shown: (a) $A_1/A_2 > 1$; (b) $A_1/A_2 \approx 1$; and (c) $A_1/A_2 < 1$. In a, spectral information from areas other than the region of interest is recorded. This is also the case in b although fewer unwanted details appear in the spectrum. In c, only information from the region of interest is recorded.

for the amylopectin peak (between 987 and 1120 cm^{-1}) than the gelatin peak (1600–1723 cm^{-1}).

Further evidence that the decrease in the amylopectin peak area at small apertures was due to diffraction effects was provided when the same experiment was repeated on a single-phase sample (25% amylopectin in D_2O). As the aperture size was reduced from 200 μm × 200 μm to below 32 μm × 32 μm, again a slight reduction in peak area was observed. This effect of a decrease in peak size at very small areas due to the loss of spectral quality and photometric accuracy has also been observed by Wopenka, Pasteris and Freeman.[18] They studied one-phase fluid inclusions (of methane and carbon dioxide) in geological specimens such as halite and found that the best (i.e. most representative) spectra were obtained provided the aperture area was about 50–70% of that of the inclusion area.

Confirmation of the dominant scale on which phase separation occurs came by taking spectra with an aperture size of 40 μm × 40 μm at positions in the gel separated by intervals of approximately 200 μm. In this way a more representative analysis of the size of phase-separated regions was generated than by relying only on the result from one position in the sample (i.e. Figure 10). The integrated areas of the amylopectin and gelatin peaks from each infrared spectrum have been plotted in vector format in Figure 12. Every spectrum, bar one, falls into either of two distinct categories—either amylopectin-rich or gelatin-rich—and provides striking evidence that the mixture consisted of phase-separated regions, with a typical size of at least 40 μm × 40 μm. Figure 12 also shows that the concentrations in the two phases were the same throughout the gel. The one point which fell between the two categories can be considered to have been one where the apertured area straddled the boundary between two phases or was centered on a phase-separated region smaller than 1600 μm^2 (40 μm × 40 μm).

Further evidence to show that the size of many of the phase-separated regions occurs on a length scale of at least 40 μm is given in the optical micrograph of Figure 13 which shows the structure of another 10% amylopectin/7% gelatin gel held in a cell made with CaF_2 windows, again formed by holding it for 25 min at 51 °C before cooling it over 45 min to 28 °C. Spherical domains held in a continuous matrix exist. These domains range in size from

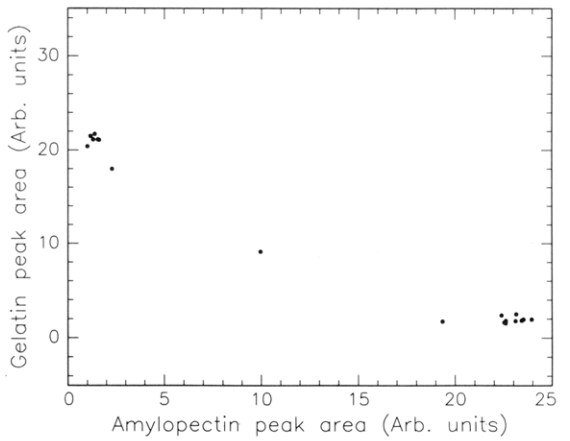

Figure 12. The integrated amylopectin (●) and gelatin (○) infrared absorption peak areas, which were measured from the spectra from 18 different 40-μm × 40-μm apertured regions in a 10% amylopectin/7% gelatin mixed gel, are shown plotted in "vector" format. The thermal history was the same as that of the sample used to generate the data shown Figure 10.

as small as 10-μm up to 150-μm diameter, although it is clear that most 40-μm × 40-μm apertured regions which are selected across the gel will be incorporated well within either the supporting phase or the inclusions of the other phase. However, since there are some inclusions which are smaller than 1600 μm^2, there will inevitably be the possibility that some 40-μm × 40-μm apertured regions contain inclusions substantially smaller than this. Figure 13 also shows that some phase-separated regions can themselves contain local phase separation on a much smaller length scale: this has been observed in agar/gelatin mixed gels[8,11] although the origin of it is unclear.

Partial Least-Squares Analysis (PLS). We now show how PLS analysis was used to convert spectral data such as the data which produced the results of Figure 12, which were only based on the measurement of peak areas, into actual concentrations. To be confident that using the PLS analysis would be accurate, we looked closely at the quality of the data in the calibration matrix. The cross-calibration method is one of the options in the PLS method and gives the errors in the predicted concentrations of each of the calibration standards compared to its actual concentration. This is done by performing a calibration on all the standards except for one and using this

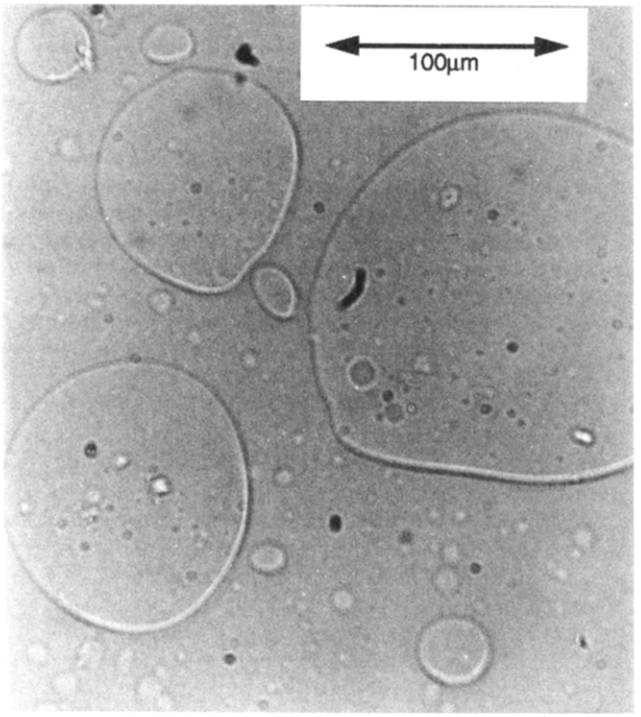

Figure 13. Optical micrograph of a 10% amylopectin/7% gelatin/83% D_2O mixed gel held between optically transparent calcium fluoride windows taken with the Jenapol optical microscope. The thermal history of the sample was the same as those used to generate Figure 10.

calibration to predict the concentration of the standard which has been left out. This procedure is then repeated for each standard in turn. The absolute errors in the concentrations of the standards for the calibration matrix, in terms of the ratio of polymer to D_2O, had standard deviations of 1.8×10^{-3}. This error compares favorably with the corresponding errors from the PLS analysis from FTIR spectroscopy,[14] where standard deviations in the errors of 1.3×10^{-3} and 6.4×10^{-3} were found for the two separate analyses carried out there. On the basis of this, a PLS analysis of spectral data was able to be carried out with confidence to predict concentration in phase-separated mixed gels. The prediction error sum of squares (PRESS) results showed that the optimum prediction occurred with a dimension of 6 for the amylopectin/D_2O component and 5 for the gelatin/D_2O component.

Concentration in the Phases of a Mixed Gel. The spectra from the 40-μm × 40-μm regions in both groupings of Figure 12 were averaged by summing the interferograms and ratioing the mean spectrum to the background of the silver chloride cell. The two mean spectra were truncated, then normalized, and scaled in the manner described in the Experimental Section. The two mean absorbance spectra were then used in the PLS analysis to predict their concentrations. The results are plotted in Figure 14 on a ternary diagram, along with a least-squares best fit for the tie line through the two points and the starting concentration. The equilibrium phase diagram (Figure 4 in ref 14) has also been plotted on Figure 14 in order that the concentrations in the mixed gel can be compared with the equilibrium concentrations of a mixture of the same concentration had been allowed to bulk phase separate. It appears that the concentrations in the two phases of this sample, within the error of the two PLS analyses, fell on the phase boundary and that therefore the concentrations in the phases had reached their equilibrium values. The tie line for this sample also fits in well with the tie lines of the equilibrium phase diagram.

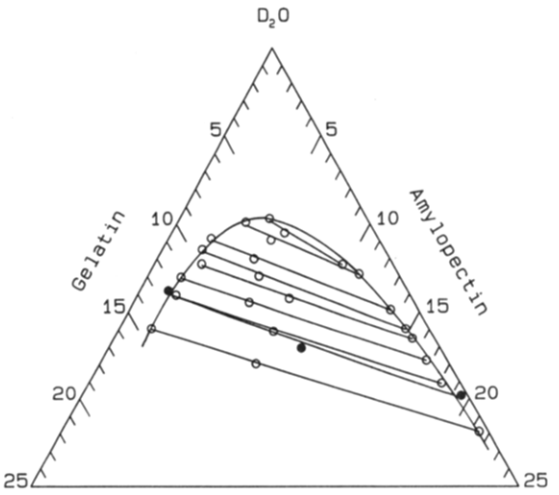

Figure 14. Ternary diagram showing the concentrations determined in the amylopectin- and gelatin-rich phase-separated domains of a mixed gel (●) as well as the starting concentration of the mixture (10% amylopectin/7% gelatin/83% D_2O) (●). The two concentrations were predicted using the partial least-squares analysis method applied to the two mean spectra averaged from the two groupings of spectra whose amylopectin and gelatin peak areas are plotted in Figure 12. A least-squares best fit tie line through the three concentrations is shown. The gel was formed by holding the sample for 25 min at 51 °C before being cooled over 45 min to 28 °C. Also shown for comparison purposes is the equilibrium phase diagram of this system at 51 °C, the experimentally determined data points which were used to generate it (○), and the tie lines through each set of three data points (Figure 4 in ref 14).

Discussion

The results of this work fall into two categories. First, we have shown that the integrated area beneath particular infrared absorption peaks from the two polymers can be used as a measure of composition in mixed biopolymer systems. Second, we have been able to predict, from spectral data, the actual concentrations in a mixed biopolymer gel using the technique of partial least-squares analysis.

By using the former integrated areas approach, tracking across a mixed solution in the two-phase region of the phase diagram (sample A) revealed fluctuations in composition across the sample. These measured fluctuations were a consequence of the locally phase-separated nature of the solution. In contrast, sample B which fell in the one-phase region showed, as expected, little variation with position. This however does not exclude the possibility that there were local inhomogeneities in composition but which, with the circular areas of 100-μm diameter over which results were taken, were too small to detect.

Again using the integrated areas approach, changes were monitored in composition with time at fixed position. No changes were apparent for one-phase samples, but two-phase samples did, on occasion, reveal dramatic fluctuations over minute intervals. These fluctuations were avoided for two-phase solutions once they were cooled to room temperature and their disappearance was attributed to gelation in the system fixing the sample in position. Since the composition in a mixed gel suffered no changes at fixed position for periods of hours, this showed that FTIR microspectroscopy experiments on gels, which take a long time, can be attempted: data collection at small areas (on the order of 40 μm × 40 μm) required acquisition times of about 0.5 h to achieve a good level of signal to noise at 8-cm^{-1} resolution.

Although we were able to observe the scale of phase separation optically by viewing samples held in CaF_2

windows, we have been able to show that FTIR microspectroscopy can be used to elucidate the scale on which phase separation takes place, even without being able to see directly the phase separation. This is particularly valuable for those systems where the phase separation cannot be optically detected. For particularly large phase-separated regions (e.g. 200 μm in diameter) the FTIR microscope could be conceivably used over a range of aperture sizes to see if the composition of a phase-separated domain varies across the domain. The estimated scale of phase separation of at least 40 μm × 40 μm for a 10% amylopectin/7% gelatin gel ties in with the optical micrograph of the same system.

Partial least-squares analysis of FTIR microspectroscopy data has been shown to be capable of determining concentrations in mixed gels. The result that the concentrations in the phase-separated regions of a mixed gel formed by holding it for 25 min at 51 °C before cooling over 45 min to 28 °C are the same as those in the bulk is important. It shows that complete demixing into two mutually insoluble components has not occurred in this case. In the model for the modulus–concentration relationship for mixed gels formulated by Clark et al.[8] and later clarified by Morris,[13] it was assumed that when gelation in a system containing two biopolymers X and Y in solution occurred, complete demixing into two distinct phases based on X and Y took place. These two concentrations lie on the boundaries of a ternary graph and connect in a straight line with the starting concentration of the solution. Clark however found that to fit the experimental data for agar/gelatin mixed gels to the theory better they were forced to abandon this assumption. Instead they argued that since the agar gelled first (because the gelation temperature of agar was higher than that of gelatin), the regions in which agar gelled did so in the absence of any gelatin. The concentration of agar was therefore simply given by the weight percentage of agar, although this adjusted concentration still lay on the boundary of a ternary graph. Apart from the fact that their theory turned out to be better fitted with this assumption, no other specific experimental evidence was cited to support this view.

Here however we observe that the concentrations in the mixed gels, for samples subject to the thermal history laid out above, at least, fell on the phase boundary i.e. complete demixing did not occur. These concentrations were therefore the same as had a sample of the same composition been allowed to phase separate to equilibrium at 51 °C. Since the bulk concentrations can be determined with FTIR spectroscopy, we have therefore shown that the concentrations in the gel can be derived directly from the equilibrium-phase diagram. It would seem that the mixed gel forms through the gelation of the liquid–liquid-phase-separated droplets which exist in the solution state, rather than it being the case that the gelation of one or the other of the polymers leads to the phase separation. However it is quite possible that solutions quenched at different rates or held for different times at the higher temperature (51 °C) before quenching may yield different results.

Conclusions

We have shown FTIR microspectroscopy to be a very valuable technique in the study of mixed biopolymer solutions and gels. It is capable of yielding a great deal of useful information which is either difficult or impossible to gather using existing techniques.

The infrared data were analyzed either in terms of the integrated areas beneath particular absorption peaks in order to estimate biopolymer composition, or in combination with the multivariate statistical analytical technique of partial least-squares analysis to predict actual concentrations from spectral data. The former approach was used to establish the spatial and temporal fluctuations in composition and also to analyze and differentiate between samples lying in the one- and two-phase regions of the equilibrium phase diagram at 51 °C. Sampling at different aperture sizes at the same position in the sample was done to estimate the scale of phase-separated domains in a mixed gel. The estimate agreed with optical microscopy on the same system. The use of PLS was found to be a viable method to determine quantitatively the concentrations in a phase-separated mixed gel and the predictive errors were of the same order of magnitude as in our earlier work with FTIR spectroscopy.[14]

In terms of mixed biopolymer gels per se we found, from the amylopectin and gelatin infrared peak areas at a succession of different positions in the sample, that the composition of the phase-separated regions fell into two distinct categories (either amylopectin-rich or gelatin-rich) and that these compositions were the same throughout the gel. We then used PLS to determine the concentrations in a 10% amylopectin/7% gelatin mixed gel's domains formed by holding the sample at 51 °C for 25 min before cooling naturally over 45 min to 28 °C and found, by comparison with the phase diagram for this system at 51 °C, that they were the same as those in a sample of the same concentration which had bulk phase separated to equilibrium.

Since FTIR was used to plot the phase diagram of the system in our earlier work, a combination of FTIR spectroscopy and FTIR microspectroscopy allows the concentrations in the mixed gel to be directly compared with equilibrium concentrations above the gelation temperature using the same molecular probe viz. infrared radiation. This clearly opens up many new avenues in the study of mixed gels which have until this point been inaccessible. In particular some of the key questions which we are now investigating include the effect of thermal history and quench rates on the concentrations and the size of the phase-separated domains in the gel. We also hope to perform compositional mapping of a mixed gel using a motorized stage. We are also conducting experiments to find out whether the PLS matrix can be used with a range of aperture sizes. This paper therefore serves to highlight how a more complete picture of the gelation of a mixed biopolymer solution may emerge with FTIR microspectroscopy. Although we have dealt with one system in particular, the approach taken throughout is of a general nature and the experiments which have been shown to be feasible with this technique should have widespread applicability.

Acknowledgment. The authors thank the Agricultural and Food Research Council for funding this work and for providing a Ph.D. studentship to Matin Durrani. We also thank Dr. David Prystupa for his infrared expertise and Dr. Allan Clark of Unilever Research for useful discussions.

References and Notes

(1) Clark, A. H.; Ross-Murphy, S. B. *Adv. Polym. Sci.* **1987**, *83*, 57–192.
(2) Ross-Murphy, S. B. In *Polymer Networks* '91; Dusek, K., Kuchanov, S. I., Eds.; VSP: Utrecht, 1992; pp 183–198.
(3) Morris, E. R. In *Food Gels*; Harris, P., Ed.; Elsevier Applied Science: London, 1990; pp 291–360.

(4) Brownsey, G. J.; Morris, V. J. In *Food Structure—Its Creation and Evaluation*; Blanshard, J. M. V., Mitchell, J. R., Eds.; Butterworths: London, 1988.
(5) Cairns, P.; Miles, M. J.; Morris, V. J. *Nature* **1986**, *322*, 89–90.
(6) Cairns, P.; Miles, M. J.; Morris, M. J. *Carbohydr. Res.* **1987**, *160*, 411–423.
(7) Fernandes, P. B.; Goncalves, M. P.; Doublier, J. L. *Carbohydr. Polym.* **1991**, *16*, 253–274.
(8) Clark, A. H.; Richardson, R. K.; Ross-Murphy, S. B.; Stubbs, J. M. *Macromolecules* **1983**, *16*, 1367–1374.
(9) Kalichevsky, M. T.; Orford, P. D.; Ring, S. G. *Carbohydr. Polym.* **1986**, *6*, 145–154.
(10) Kalichevsky, M. T.; Ring, S. G. *Carbohydr. Res.* **1987**, *162*, 323–328.
(11) Horiuchi, H.; Sugiyama, J. *Agric. Biol. Chem.* **1987**, *51*, 2171–2176.
(12) Doi, K. *Biochim. Biophys. Acta* **1965**, *94*, 557–565.
(13) Morris, E. R. *Carbohydr. Polym.* **1992**, *17*, 65–70.
(14) Durrani, C. M.; Prystupa, D. A.; Donald, A. M.; Clark, A. H. *Macromolecules* **1993**, *26*, 981–988.
(15) *Infrared Microspectroscopy: Theory and Applications*; Messerschmidt, R. G., Harthcock, M. A., Eds.; Marcel Dekker: New York, 1988; Vol. 5.
(16) Krishnan, K.; Hill, S. L. In *Infrared Microspectroscopy: Theory and Applications*; Ferraro, J. R., Krishnan, K., Eds.; Academic Press: London, 1990; pp 103–165.
(17) Harthcock, M. A.; Atkin, S. C. *Appl. Spectrosc.* **1988**, *42*, 449–445.
(18) Wopenka, B.; Pasteris, J. D.; Freeman, J. J. *Geochim. Cosmochim. Acta* **1990**, *54*, 519–533.
(19) Ring, S. G.; Colonna, P. C.; I'Anson, K. J.; Kalichevsky, M. T.; Miles, M. J.; Morris, V. J.; Orford, P. D. *Carbohydr. Res.* **1987**, *162*, 277–293.
(20) Djabourov, M. *Contemp. Phys.* **1988**, *29*, 273–297.
(21) Messerschmidt, R. G. In *Infared Microspectroscopy: Theory and Applications*; Messerschmidt, R. G., Harthcock, M. A., Eds.; Marcel Dekker: New York 1988; pp 1–19.
(22) Marcott, C.; Laughlin, R. G.; Sommer, A. J.; Keaton, J. E. In *FTIR Spectroscopy in Colloid and Interface Science*; Scheuing, D. R., Ed.; American Chemical Society: Washington, DC, 1991; pp 71–86.
(23) Johansson, G.; Joelsson, M.; Bastos, M. *Polymer* **1992**, *33*, 152–155.
(24) Prystupa, D. A. Personal communication.